Journal of Biomolecular NMR, **21:** 367–372, 2001.
KLUWER/ESCOM

Transverse relaxation optimized HCN experiment for nucleic acids: Combining the advantages of TROSY and MQ spin evolution

Bernhard Brutscher* & Jean-Pierre Simorre
Institut de Biologie Structurale, Jean-Pierre Ebel C.N.R.S.-C.E.A., 41, rue Jules Horowitz, 38027 Grenoble Cedex, France

Received 30 July 2001; Accepted 1 October 2001

Key words: HCN, multiple quantum coherence, NMR assignment, nucleic acids, triple resonance, TROSY

Abstract

A three-dimensional MQ-TROSY-HCN pulse sequence is presented which provides intra-base and sugar-to-base correlations for ^{13}C, ^{15}N labeled nucleic acids (RNA, DNA). The experiment simultaneously exploits the favorable relaxation properties of ^{1}H-^{13}C multiple quantum coherence for sugar carbons and of ^{13}C TROSY-type spin evolution for base carbons. MQ-TROSY-HCN thus combines the advantages of MQ-HCN for sugar-to-base and TROSY-HCN for intra-base correlations in a single experiment. In addition, two slightly different implementations of the MQ-TROSY-HCN experiment ensure optimal performance for small and larger oligonucleotides, respectively. The advantages of the MQ-TROSY-HCN experiment compared to the best previous implementations of HCN are demonstrated for a 33 nucleotide RNA aptamer.

The triple resonance HCN experiment (Sklenár et al., 1993) correlates the sugar $H_{1'}$ and the base H_6/H_8 protons of the same nucleotide via the shared N_9/N_1 of the glycosidic bonds. HCN is a crucial experiment for sequential assignment of nucleic acids as it allows the unambiguous distinction between intra- and inter-nucleotide sugar-base correlations observed in ^{13}C filtered ^{1}H-^{1}H NOESY spectra (Nikonowicz and Pardi, 1993; Brutscher et al., 2001). Due to the small heteronuclear ^{13}C-^{15}N scalar couplings ($^{1}J_{CN} \leqslant 12$ Hz), the sensitivity of this experiment is reduced by spin relaxation during the long ^{13}C→^{15}N transfer delays. Application of the originally proposed pulse scheme is therefore limited to small oligonucleotides. Recently it has been demonstrated that the sensitivity of the HCN experiment can be significantly enhanced. Two complementary experimental approaches have been developed which exploit the favorable relaxation properties of either multiple-quantum (MQ) coherence (Griffey and Redfield, 1987) or single-transition spin states, the so-called TROSY effect (Pervushin et al., 1997). In the following we will refer to these experiments as MQ-HCN and TROSY-HCN, respectively. In the MQ-HCN experiment, originally proposed by Marino et al. (1997) and later optimized by Fiala et al. (1998), the spin system evolves as a ^{1}H-^{13}C MQ (superposition of zero-quantum and double-quantum) coherence during the ^{13}C→^{15}N transfer delays. For molecules in the slow tumbling regime, MQ spin evolution largely eliminates the ^{1}H-^{13}C dipolar contribution to spin relaxation (Griffey and Redfield, 1987; Bax et al., 1989; Grzesiek and Bax, 1995). Despite additional relaxation pathways with remote proton spins, MQ-HCN proved to produce a significant sensitivity improvement with respect to the originally proposed single-quantum (SQ) version of HCN (Marino et al., 1997; Fiala et al., 1998; Sklenár et al., 1998). To refocus ^{1}H-^{1}H scalar coupling evolution of the ^{1}H-^{13}C MQ coherence, separate experiments need to be recorded for the intra-base and sugar-to-base correlations, which decreases the effective sensitivity gain by a factor of $\sqrt{2}$. The TROSY-HCN experiment (Fiala et al., 2000; Riek et al., 2001) exploits the favorable relaxation properties of single-transition spin states of ^{1}H-coupled ^{13}C spins during the ^{13}C→^{15}N coherence

*To whom correspondence should be addressed. E-Mail: Bernhard.Brutscher@ibs.fr

transfer. Relaxation of one of the single-transition spin states (doublet lines) is reduced due to cross correlation between the ^{13}C chemical shift anisotropy (CSA) and the ^{13}C-^{1}H dipolar interaction (Brutscher, 2000). In addition, Riek et al. (2001) have shown that the signal loss during the transfer delay is further reduced by cross-correlation of the C_6 ($C_{1'}$) CSA and the C_6-C_5 ($C_{1'}$-$C_{2'}$) dipolar interactions. Contrary to MQ-HCN, the TROSY-HCN experiment is optimized simultaneously for the sugar- and base-moieties.

Whether MQ-HCN or TROSY-HCN will provide better sensitivity depends on the relative contribution of ^{13}C CSA and ^{13}C-^{1}H dipolar interactions to the ^{13}C SQ relaxation rate. For a small CSA contribution MQ-HCN is expected to yield better results, whereas in the case of a similar contribution from CSA and dipolar relaxation TROSY-HCN should be used. As CSA – induced relaxation is proportional to the magnetic field strength ($\propto B_0$) the results will also be dependent on the available magnetic field. Fiala et al. (2000) have computed relaxation rates for SQ, MQ, and TROSY-type spin evolution of C_6, C_8 base and $C_{1'}$ sugar carbons as a function of magnetic field ranging from 500 to 1000 MHz ^{1}H frequency. Within this range, the smallest relaxation rates are found for TROSY-type spin evolution in the case of C_6 and C_8 base carbons, whereas for $C_{1'}$ sugar carbons MQ spin evolution is clearly preferable to TROSY-type spin evolution.

Here we present a new pulse sequence which combines the favorable properties of MQ coherence for the sugar carbons with the advantages of TROSY for the base carbons. The sequence, which we will refer to as MQ-TROSY-HCN is shown in Figure 1. The sequence is basically derived from the TROSY-HCN sequence of Riek et al. (2001), where the ^{13}C→^{15}N 'out and back' transfer is achieved in a HMQC fashion (between time points 'b' and 'd'). The sequence before time point 'b' creates MQ ^{1}H-^{13}C coherence for the sugar moieties and SQ coherence for the base moieties. In the last part (d–f) these coherences are reconverted into detectable ^{1}H coherence. In short, the coherence transfer pathways for the sugar-to-base and intra-base correlations in product operator notation (Sørensen et al., 1983) are as follows: the sequence starts with selective excitation of $H_{6,8}$ base protons. The inphase coherence H_y is then transferred into antiphase coherence $2H_xC_z$ by a subsequent INEPT transfer. The following non-selective ^{1}H 90° pulse simultaneously restores the base magnetization along the z axis and turns the sugar magnetization in the transverse plane. At time point 'a' the spin system is thus described by $\sigma_a^{base} = 2H_zC_z$ for the base moieties and by $\sigma_a^{sugar} = H_x$ for the sugar moieties. During the subsequent delay Δ_2 antiphase $2H_yC_z$ coherence is created for the sugar moieties. After the ^{13}C excitation pulse at time point 'b' the sugar moieties are in a MQ state $\sigma_b^{sugar} = 2H^+C_y$, whereas the base moieties are in the SQ state $\sigma_b^{base} = u2H_zC_y + vC_y$, where the scalar factors 'u' and 'v' denote the relative contributions from ^{1}H and ^{13}C steady state magnetization, respectively (Brutscher et al., 1998; Pervushin et al., 1998). σ_b^{base} can be rewritten as a linear combination of two single-transition states $\sigma_b^{base} = (u + v)H^{\beta}C_y + (u - v)H^{\alpha}C_y$, with $H^{\beta}C_y$ representing the slowly relaxing ^{13}C doublet line. Note that the relative sign of 'u' and 'v' is determined by the phase φ_1 which should be adjusted experimentally to $\varphi_1 = y$ or $\varphi_1 = -y$ (spectrometer dependent) to enhance the slowly relaxing $H^{\beta}C_y$ spin state. No radiofrequency (RF) pulses are applied during the ^{13}C→^{15}N HMQC transfer (b–d) on the $H_{6,8}$ base protons to allow for TROSY-type relaxation enhancement. Chemical shift evolution is refocused by band-selective central 180° pulses simultaneously applied to the $H_{1'}$, $C_{1'}$, and $C_{6,8}$ resonances. The selective character of these pulses also ensures refocusing of spin evolution due to the scalar carbon-carbon couplings $J_{C6C5} \approx 67$ Hz, $J_{C1'C2'} \approx 43$ Hz, $J_{C8C6/5/4} \approx 8$–11 Hz, and $J_{C6C2} \approx 2$–3 Hz (Wijmenga and van Buren, 1998). As the $H_{1'}$ spectral region overlaps with the H_5 base region additional band-selective 180° pulses applied to the $H_{1'}$ (H_5) band were added in the middle of the ^{13}C→^{15}N transfer delays T to refocus the small scalar couplings $J_{C6H5} \approx 4$–5 Hz. ^{13}C chemical shift labeling is obtained in a constant time (CT) manner by the time-proportional simultaneous shift of a ^{13}C and a ^{15}N 180° pulse. At time point 'c' ^{15}N transverse coherence is created for frequency labeling of the N_9/N_1 chemical shifts. At time point 'e' the spin system has returned to the state of time point 'a' ($\sigma_e^{base} = \sigma_a^{base}$, $\sigma_e^{sugar} = \sigma_a^{sugar}$). The final INEPT step transfers the two-spin order $2H_zC_z$ of the base carbons into an inphase coherence H_y, and the ^{1}H 90° pulse prior to detection converts the spin state of the sugar moieties into a detectable $\sigma_f^{sugar} = \pm H_x$ coherence without changing the spin state of the base moieties $\sigma_f^{base} = H_y$. During acquisition sugar and base protons will evolve with a relative phase shift of 90°. To obtain pure absorption line shapes in the ^{1}H dimension for both sugar-to-base and intra-base correlations two data sets are recorded with different phase settings of φ_4:

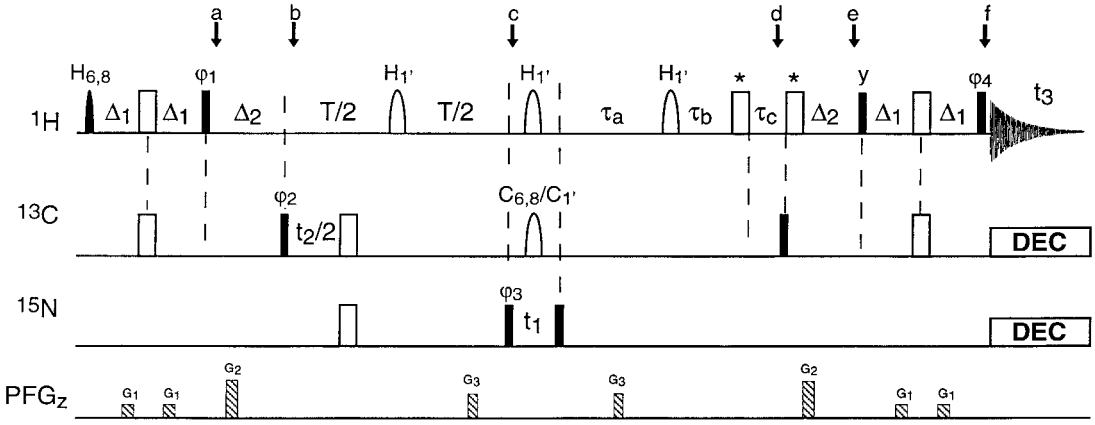

Figure 1. Pulse sequence for 3D MQ-TROSY-HCN experiment of nucleic acids. The 180° ^{1}H pulses marked by a star are omitted for the standard version of MQ-TROSY-HCN and the delays τ_a, τ_b, and τ_c are set to $\tau_a = T/2$, $\tau_b = T/2$, and $\tau_c = 0$. A J_{CH} decoupled (t_2) version of MQ-TROSY-HCN is obtained by addition of the two 180° ^{1}H pulses marked by a star and setting the delays τ_a, τ_b, and τ_c to $\tau_a = (T-t_2)/2$, $\tau_b = T/2$, and $\tau_c = t_2/2$. The carrier frequencies were set to 4.7 ppm (^{1}H), 112 ppm (^{13}C), and 153ppm (^{15}N). All RF pulses are applied along the x axis unless indicated. Non-selective 90° and 180° RF pulses are represented by filled and open bars, respectively. Band-selective 90° and 180° RF pulses are represented by filled and open shaped pulse symbols. The 90° excitation pulse applied to the $H_{6,8}$ frequency band was applied with an ESNOB profile centered at 7.8 ppm and covering a band width of 2.2 ppm (pulse length of 1.05 ms at 600 MHz). The $H_{1'}$ refocusing pulses have a RSNOB shape centered at 5.6 ppm and covering a band width of 1.4 ppm (pulse length of 2.20 ms at 600 MHz). SNOB pulses (Kupče et al., 1995) were chosen because of their short pulse length for a given band width. For selective ^{13}C refocusing during t_1 two band-selective pulses with REBURP profile (Geen and Freeman, 1991) were centered at 140 ppm for the $C_{6,8}$, and at 90 ppm for the $C_{1'}$, carbons, both covering a band width of 12 ppm (pulse length of 2.69 ms at 150 MHz). The two pulses are then superposed to a single shaped pulse (Kupče and Freeman, 1993). The transfer delays are set to $\Delta_1 = 1/4J_{C_{6,8}H_{6,8}}$, $\Delta_2 = 1/2J_{C_{1'}H_{1'}}$, and $T = 1/2J_{NC}$. For the present application they were optimized to $\Delta_1 = 1.25$ ms, $\Delta_2 = 2.80$ ms, and T = 30 ms. The phase φ_1 is adjusted to either $\varphi_1 = y$ or $\varphi_1 = -y$, depending on the spectrometer, to yield maximal sensitivity. Pulsed field gradients G_1, G_2, and G_3, are applied along the z-axis (PFG_z) with a gradient strength of approximately 20 G/cm and pulse lengths ranging from 100 to 500 μs, followed by a recovery delay of 100 μs. A two-step phase cycle is applied with $\varphi_3 = x, -x$ and the receiver phase $\varphi_{rec} = x, -x$. Quadrature detection in the ^{13}C (t_2) and ^{15}N (t_1) dimensions is achieved by incrementing the phases φ_2 (t_2) and φ_3 (t_1),respectively, according to the STATES method. Two data sets are recorded with the phase φ_4 set to $\varphi_4 = y$ and $\varphi_4 = -y$. The recorded data sets are then added or subtracted to yield the intra-base or sugar-to-base HCN correlations, respectively. The pulse sequence code in VARIAN language is available from the authors upon request.

(A) $\varphi_4 = y$ and (B) $\varphi_4 = -y$. Addition (A+B) and subtraction (A−B) of the two data sets yields subspectra containing either the sugar-to-base or the intra-base correlations which can then be phased separately to account for the 90° phase shift.

The performance of the different HCN experiments is demonstrated on a 1 mM sample of an ^{13}C, ^{15}N labeled RNA aptamer of 33 nucleotides in a 1:1 complex with theophylline (Zimmermann et al., 1997). 2D H(C)N correlation spectra acquired with the TROSY-HCN (Riek et al., 2001) and MQ-HCN (Fiala et al., 1998) pulse sequences are shown in Figures 2A and 2B, respectively. The MQ-HCN experiment optimized for sugar-to-base correlations yields on average a three-fold signal enhancement compared to TROSY-HCN with a maximal gain of a factor of nine for nucleotide C8. This result confirms predictions from ^{13}C CSA calculations (Fiala et al., 2000), and further supports the idea of combining the advantages of MQ and TROSY spin evolution for the sugar and base moieties in a single experiment. As both, intra-base and sugar-to-base HCN correlations are required for an NMR assignment, the sensitivity of the new MQ-TROSY-HCN experiment may be best compared to the sum of a TROSY-HCN and a MQ-HCN spectrum (Figure 3A), where each individual experiment is acquired in half the experimental time used for the MQ-TROSY-HCN experiment shown in Figure 3B. A quantitative evaluation of the cross peak intensities in the spectra of Figures 3A and 3B shows that MQ-TROSY-HCN yields on average a sensitivity gain of 30% for sugar-to-base correlations and of 60% for intra-base correlations. Exceptions are the sugar-to-base correlations detected for nucleotides G11, C22, U23, and C27, for which the peak intensities detected in the MQ-TROSY-HCN spectrum are only 80% (G11), 55% (C22), 25% (U23) and 44% (C27) of the intensities observed in the spectrum of Figure 3A. The reason for the poor performance of MQ-TROSY-HCN for a small number of sugar-to-

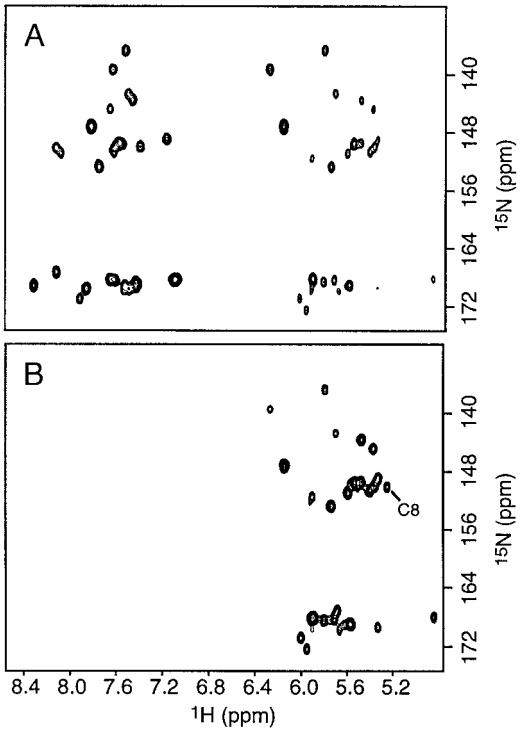

Figure 2. 2D H(C)N correlation spectra recorded on a 1mM sample of the 33 nucleotide RNA aptamer-theophylline complex in D_2O at 600 MHz ^{1}H frequency and 298 K sample temperature. The spectra were acquired using a (A) TROSY-HCN (Riek et al., 2001), and a (B) MQ-HCN (Fiala et al., 1998) experiment. Data sets of 512 (^{1}H) × 40 (^{15}N) complex points were recorded for spectral width of 7000 Hz (^{1}H) × 2700 Hz (^{15}N) in an experimental time of 3 h per experiment.

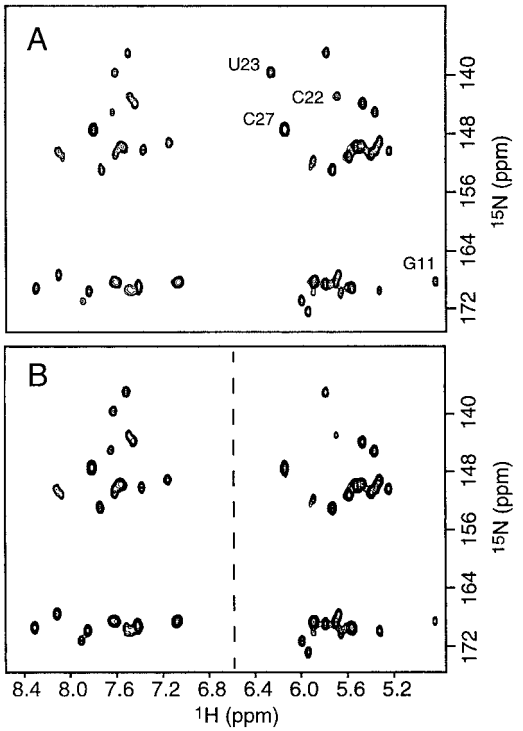

Figure 3. 2D H(C)N correlation spectra recorded on a 1 mM sample of the 33 nucleotide RNA aptamer -theophylline complex in D_2O at 600 MHz ^{1}H frequency and 298 K sample temperature. (A) Sum of a TROSY-HCN and a MQ-HCN spectrum, each recorded in an experimental time of 1.5 h. (B) MQ-TROSY-HCN spectrum acquired in an experimental time of 3 h. This spectrum is the combination of two sub-spectra obtained for the base and sugar regions as explained in the text. Data sets of 512 (^{1}H) × 40 (^{15}N) complex points were recorded for spectral width of 7000 Hz (^{1}H) × 2700 Hz (^{15}N).

base HCN correlations is most likely the increased number of band-selective RF pulses. For example, the $H_{1'}$ sugar protons of G11, U23, and C27 resonate at the edge of the band width covered by the 180° $H_{1'}$ refocusing pulses. A rather narrow $H_{1'}$ band width is required for the MQ-TROSY-HCN experiment in order to avoid perturbation of the $H_{6,8}$ resonances. As the performance of band-selective RF pulses increases with the magnetic field strength (Brutscher et al., 2001), we expect that MQ-TROSY-HCN will compare even more favorably at higher magnetic field strength (e.g., 800 MHz ^{1}H frequency) using a slightly increased $H_{1'}$ band width.

Additional frequency labeling of the $C_{6,8}$ and $C_{1'}$ chemical shifts provides the required high spectral resolution for application of the HCN experiment to larger oligonucleotides. This is achieved in a CT manner by the MQ-TROSY-HCN pulse sequence of Figure 1. Contrary to the TROSY-HCN pulse scheme of Riek et al (2001) ^{13}C spin evolution due to the one-bond scalar couplings $^1J_{C6C5}$ and $^1J_{C1'C2'}$ is refocused during the incremented time period t_2, and only the small heteronuclear two-bond coupling $^2J_{C6H5}$ remains active during t_2. This allows recording of 3D spectra with high resolution along the ^{13}C dimension ($t_2^{max} \leqslant 2T \approx 60$ ms). To illustrate the use of 3D MQ-TROSY-HCN Figure 4B shows strips taken along the ω_1 (^{15}N) dimension of a 3D spectrum recorded on the 33 nucleotide RNA test sample. Correlations between the ribose $H_{1'}$-$C_{1'}$and the base $H_{6,8}$-$C_{6,8}$ moieties are established via the N_1/N_9 chemical shifts. During t_2 the base carbons evolve as a superposition of two single-transition spin states as explained above. As no *active* spin-state-selection is performed two correlation peaks may be observed in the 3D spectrum along the ^{13}C dimension at $\omega_C \pm \pi J_{CH}/2$. The intensity of the fast relaxing doublet peak will however be significantly reduced by spin relaxation during the long $^{13}C \rightarrow {}^{15}N$ transfer delays and by the combined

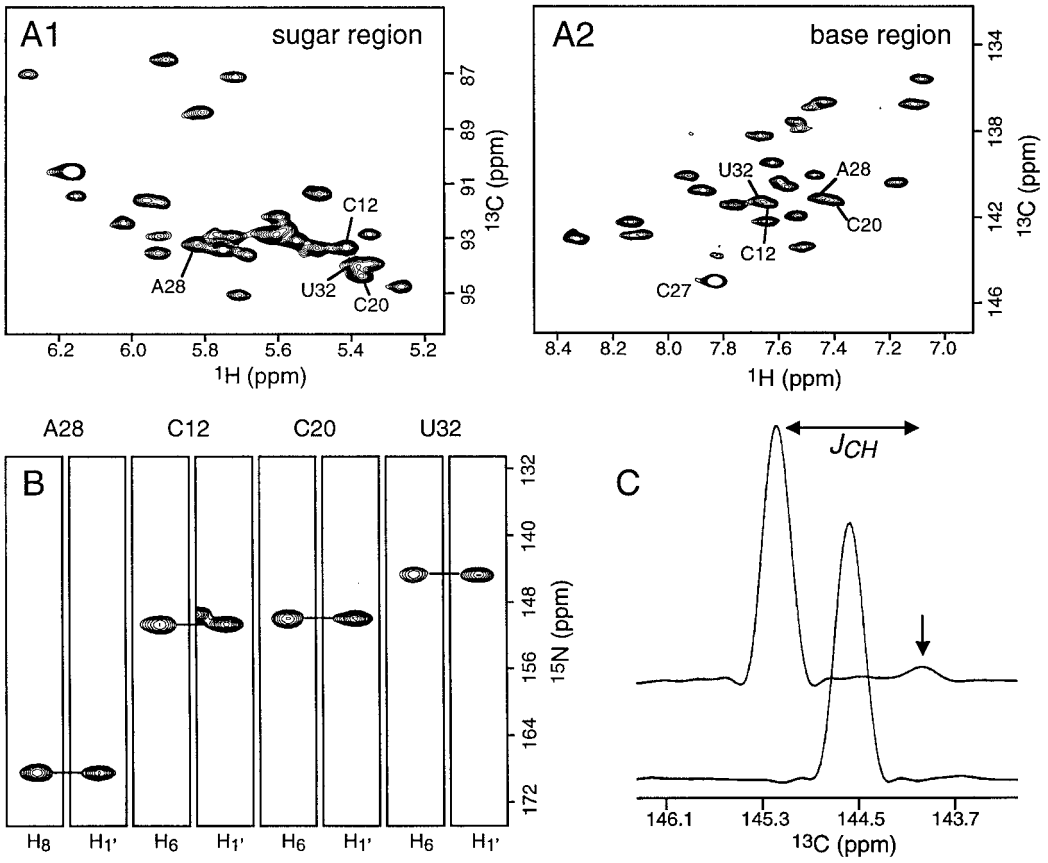

Figure 4. 2D (^{1}H,^{13}C) projection of the sugar (A1) and base (A2) regions of a 3D MQ-TROSY-HCN spectrum recorded with the pulse sequence of Figure 1 on a 1 mM sample of the 33 nucleotide RNA aptamer-theophylline complex in D_2O at 600MHz ^{1}H frequency and 298 K sample temperature. Two data sets (with phase settings $\varphi_4 = y$ and $\varphi_4 = -y$) of 512 (^{1}H) × 40 (^{15}N) × 150 (^{13}C) complex points were recorded for spectral width of 7000 Hz (^{1}H) × 2700 Hz (^{15}N) × 3000 Hz (^{13}C) in an experimental time of 30 h. The ^{1}H-^{13}C correlation peaks belonging to the sugar and base moieties of the same nucleotide can be assigned via the N_9/N_1 chemical shifts. This is illustrated in (B) for residues A28, C12, C20, and U32 using strips extracted from the 3D MQ-TROSY-HCN spectrum along the ^{15}N dimension. (C) A small residual doublet peak is detected in the ^{13}C dimension for nucleotide C27 as highlighted by an arrow in the upper 1D spectrum. As explained in the text no residual peaks are detected in the J_{CH} decoupled (t_2) version of MQ-TROSY-HCN. The lower 1D spectrum shows the corresponding ^{13}C trace of C27 extracted from a J_{CH} decoupled (t_2) MQ-TROSY-HCN spectrum recorded under identical experimental conditions.

use of ^{1}H and ^{13}C steady state magnetization which enhances one of the doublet peaks and partially suppresses the other. The degree of suppression depends on the relative contributions from ^{1}H and ^{13}C steady state magnetization. For u=v complete suppression is obtained, whereas if 'u' is different from 'v' a residual doublet peak may be detected in the spectrum. It has been shown for nucleic acids that $|u| \approx |v|$ if optimized recycle delays are used (Brutscher et al., 1998). In the case of our 33 nucleotide RNA aptamer the intensity of all residual doublet peaks is reduced beyond detection except for nucleotide C27 (Figure 4C), which has been shown to undergo fast time scale internal mobility (Zimmermann et al., 1998; Boisbouvier et al., 1999). The small residual peak detected for the C_6 of this nucleotide, however, does not affect interpretation of the 3D MQ-TROSY-HCN spectrum.

Higher intensities of the residual doublet components are expected for smaller molecules where differential relaxation of the two lines is less pronounced, or for systems with very unequal relative contributions from ^{1}H and ^{13}C steady state magnetization. In these situations it will be advantageous to use a slightly modified version of the 3D MQ-TROSY-HCN experiment which decouples the $H_{6,8}$ protons from the $C_{6,8}$ carbons during t_2 spin evolution (J_{CH} decoupled (t_2) MQ-TROSY-HCN). This is experimentally realized by adding two 180° ^{1}H pulses marked by a star

in Figure 1, and by changing the delays τ_a, τ_b, and τ_c to their corresponding values given in Figure 1. As a consequence the HCN correlation peaks of the base moieties detected with this J_{CH} decoupled (t_2) version of the MQ-TROSY-HCN experiment are no longer shifted by $+\pi J_{CH}/2$ along the ^{13}C dimension, but detected at the Larmor frequency ω_C of the involved base carbon. This is illustrated by 1D traces extracted from 3D MQ-TROSY-HCN spectra along the ^{13}C dimension for nucleotide C27 (Figure 4C). The upper spectrum was recorded without ^1H decoupling during t_2, whereas the lower spectrum was obtained using the pulse sequence including the modifications explained above. A drawback of the J_{CH} decoupled (t_2) version is the loss of the CT character of the ^{13}C frequency labeling as TROSY line narrowing is now only effective during the delay ($2T-t_2$). The signal attenuation during t_2 induces a small sensitivity loss with respect to the *non-*J_{CH} decoupled (t_2) MQ-TROSY-HCN version. For small nucleic acids, however, this sensitivity loss is compensated by the addition of the two doublet components.

In conclusion, the new 3D MQ-TROSY-HCN experiment provides intra-nucleotide correlations between the sugar $H_{1'}$ and the base H_6/H_8 protons required for sequential assignment of nucleic acids. MQ-TROSY-HCN combines the advantages of MQ-HCN for the sugar moieties and TROSY-HCN for the base moieties in a single experiment. This approach yields significantly increased sensitivity with respect to currently available alternative strategies for most of the nucleotides. Two slightly different implementations of the MQ-TROSY-HCN experiment are proposed: the J_{CH} decoupled (t_2) version of MQ-TROSY-HCN ensures optimal performance for small oligonucleotides, whereas the standard (*non-*J_{CH} decoupled) version should be preferred for larger molecular systems. The concept of transverse relaxation optimization by simultaneously exploiting the properties of MQ coherences and single transition spin states may be equally useful for other NMR experiments where different coherence transfer pathways are detected simultaneously. An example is the recently introduced bid-HCNCH experiment (Hu et al., 2001) for nucleic acids. Implementation of a MQ-TROSY type version of this experiment is currently under investigation in our laboratory.

Acknowledgements

The authors thank Drs Art Pardi and Grant Zimmermann (University of Colorado) for the preparation of the $^{13}C,^{15}N$ labeled theophylline-binding RNA aptamer. This work was supported by the Commissariat à l'Energie Atomique, the Centre National de la Recherche Scientifique (France), and Molecular Simulations Inc. (San Diego, CA).

References

Bax, A., Kay, L.E., Sparks, S.W. and Torschia, D.A. (1989) *J. Am. Chem. Soc.*, **111**, 408–409.

Boisbouvier, J., Brutscher, B., Simorre, J.-P. and Marion, D. (1999) *J. Biomol. NMR*, **14**, 241–252.

Brutscher, B. (2000) *Conc. Magn. Reson.*, **12**, 207–229.

Brutscher, B., Boisbouvier, J., Kupče, E., Tisné, C., Dardel, F., Marion, D. and Simorre, J.-P. (2001) *J. Biomol. NMR*, **19**, 141–151.

Brutscher, B., Boisbouvier, J., Pardi, A., Marion, D. and Simorre, J.-P. (1998) *J. Am. Chem. Soc.*, **120**, 11845–11851.

Fiala, R., Jiang, F. and Sklenár, V. (1998) *J. Biomol. NMR*, **12**, 373–383.

Fiala, R., Czernek, J. and Sklenár, V. (2000) *J. Biomol. NMR*, **16**, 291–302.

Geen, H. and Freeman, R. (1991) *J. Magn. Reson.*, **93**, 93–141.

Griffey, R.H. and Redfield A.G. (1987) *Quart. Rev. Biophys.*, **19**, 51–82.

Grzesiek, S. and Bax, A. (1995) *J. Biomol. NMR*, **6**, 335–339.

Hu, W., Gosser, Y.Q., Xu, W. and Patel, D.J. (2001) *J. Biomol. NMR*, **167**, 167–172.

Kupče, E. and Freeman, R. (1993) *J. Magn. Reson.*, **105A**, 234–238.

Kupče, E., Boyd, J. and Campbell, I.D. (1995) *J. Magn. Reson.*, **106B**, 300–303.

Marino, J.P., Diener, J.L., Moore, P.B. and Griesinger, C. (1997) *J. Am. Chem. Soc.*, **119**, 7361–7366.

Nikonowicz, E.P. and Pardi, A. (1993) *J. Mol. Biol.*, **232**, 1141–1156.

Pervushin, K., Riek, R., Wider, G. and Wüthrich, K. (1997) *Proc. Natl. Acad. Sci. USA*, **94**, 12366–12371.

Pervushin, K., Riek, R., Wider, G. and Wüthrich, K. (1998) *J. Am. Chem. Soc.*, **120**, 6394–6400.

Riek, R., Pervushin, K., Fernández, C., Kainosho, M. and Wüthrich, K. (2001) *J. Am. Chem. Soc.*, **123**, 658–664.

Sklenár, V., Dieckmann, T., Butcher, S.E. and Feigon, J. (1998) *J. Magn. Reson*, **130**, 119–124.

Sklenár, V., Peterson, R.D., Rejante, M.R. and Feigon, J. (1993) *J. Biomol. NMR*, **3**, 721–727.

Sørensen, O.W., Eich, G.W., Levitt, M.H., Bodenhausen, G. and Ernst, R.R. (1983) *Prog. NMR Spectrosc.*, **16**, 163–192.

Wijmenga, S.S. and van Buren B.N.M. (1997) *Prog. NMR Spectrosc.*, **32**, 287–387.

Zimmermann, G.R., Jenison, R.D., Wick, C.L., Simorre, J.-P. and Pardi, A. (1997) *Nat. Struct. Biol.*, **4**, 644–649.

Zimmermann, G.R., Shields, T. P., Jenison, R.D., Wick, C.L. and Pardi, A. (1998) *Biochemistry*, **37**, 9186–9192.